

# Genetic Algorithm to Inverse Least Squares Comparative Dual Optimization for Ceramic Hip Arthroplasty in Medical Physics

Francisco Casesnoves

PhD Engineering, MSc Physics, Physician. Independent Research Scientist. International Association of Advanced Materials, Sweden. Uniscience Global Scientific Member, Wyoming, USA. Harjumaa, Estonia.

## ABSTRACT

### Article Info

Volume 8, Issue 1

Page Number : 88-108

### Publication Issue :

January-February-2022

### Article History

Accepted : 01 Jan 2022

Published : 22 Jan 2022

Ceramic THA constitutes an important group among the most frequent used implants in Biomedical Engineering and Medical Devices research field. A genetic algorithms computational nonlinear optimization is presented with two commonly ceramic materials for Ceramic-on-Ceramic (CoC) THA. This optimization is compared to a previously published Inverse Least\_Squares one. Selected materials are Alumina ( $Al_3O_2$ ), and Zirconium ( $ZrO_2$ ). Principal result is the numerical validation-verification of the K adimensional-constant parameter of the model with both methods. Results from previous Least-Squares algorithm and Genetic Algorithms show be closely with identical magnitude order. Numerical figures for both dual optimizations give acceptable model-parameter values with low residuals. These findings are demonstrated with series of 2D and 3D Graphical/Interior Optimization graphics also. 4D Interior Optimization method constitutes also the computational innovation of this study. The Genetic Algorithms dual-optimized ceramic-model parameters are mathematically proven/verified. Mathematical consequences are obtained for model improvements and *in vitro* simulation methodology. These confirmed wear parameters for *in vitro* determinations and efficacious Genetic Algorithms approach constitute the article novelty of both optimization methods. Results for *in vitro* tribotesting wear predictions with these parameters for laboratory experimental show be useful/effective. Applications for clinical Medical Physics and Bioengineering improvements in material/ceramic-THA and CAM constitute practical consequences.

**Keywords :** Inverse Least Squares (ILS), Genetic Algorithms (GA), Tikhonov Regularization, (TR), Software Engineering Methods, Genetic Algorithm Nonlinear Optimization, Artificial Implants (AI), CAD (Computer Aided Design), CAM (Computer Aided Manufacturing), (Hip Implants, Total Hip Arthroplasty (THA), CoC (Ceramic on Ceramic implant), Objective Function (OF), Prosthesis Materials, Wear, Biomechanical Torques/Forces.

## I. INTRODUCTION

In a series of previous contributions, THA wear in vitro predictions CoC and MoM were modelled and optimized [1-4] with Inverse  $L_2$  Least Square methods. Main results comprised an accurate adimensional model parameter  $K$ . Programming methods and software design for Numerical and 2D-3D Graphical/Interior Optimization were presented [1-5], with new development of 4D Graphical/Interior Optimization.

This study is focused on validation of all Dual CoC results obtained with Inverse  $L_2$  Least Square methods by using Genetic Algorithms Optimization. Both methods are compared and evaluated each other. The selected model from [1-4] shows a number of mathematical characteristics as follows,

Lemma 1 [Casesnoves, 2019].- Unless constraints are set, inexistence of global minimum holds when optimizing the model [1-4],

$$W = K \frac{L \times X}{H} ;$$

Proof:

given the tribological model,

$$W = K \frac{L \times X}{H} ;$$

hence,

$$H \bullet W = K \bullet L \bullet X ; \tag{1}$$

the left side member has two parameters and the right side three, theoretically all of them  $\in (-\infty, \infty)$ , open interval. The equality has infinite solutions, either positive and/or negative options, unless strict constraints are set for at least a number of these parameters. That is, to convert the unbounded equality for a series of values into a system of equations with unique/multiple-limited solution(s).

The ILS method used in previous contributions [51], is based on Tikhonov Regularization Theory, selecting a Matlab appropriate development

subroutine. The main difficulty of ILS and TR is the ill-posed matrices possibility. However, modern programming systems subroutines usually sort this hurdle with an automatic set-in technique, such as singular values decomposition and others. In general [51] ILS with  $L_2$  norm sets as Tikhonov Functional that reads,

minimize functional  $J(\alpha)$ ,

$$J_{\alpha}(u)_{u \in \mathcal{R}} = \|Au - E\|_2^2 + \alpha J(u); \tag{2}$$

where first term in the Functional Principal Term, in this study  $Au$  is the model matrix-vector data,  $E$  is the wear experimental data matrix. In second term multiplied by  $\alpha$  is the Regularization Parameter. That is,  $J(u)$  is the regularization functional term usually related to smoothness, sparsity and other specific characteristics of the  $J_{\alpha}(u)$ . Norms are set  $L_2$ . Instead  $R$  Space, Hilbert Spaces or  $C$  ones can be used to define functionals also. Since Matlab subroutines have incorporated smoothness, it is taken  $\alpha = 0$  for this study. This Tikhonov functional, expressed simpler, was developed in previous contributions [1-4] with acceptable results.

GA method is a stochastic optimization method different than ILS. GA is based on the Darwinist natural species selection. The species whose genetic code results successful in survival and adaptation on environment are chosen. At every step, a refinement is made, discarding the genetic codes that do not fit the constraints. This process lasts until convergence is reached. There are variants of GA methods. They have in common the steps of selection, mating, mutation and final convergence. Binary GA method is based on a binary discrete code (for example, black or white skin in persons), base-two numerals. Continuous GA method uses continuous variables. The difference between them is that Binary GA uses decode of chromosomes and evaluates the cost for

every chromosome at initial stages. In this study, Continuous GA method is applied. The OF for GA optimization in this research is,

$$\begin{aligned} & \text{minimize functional } J(\alpha), \\ & \text{with } \alpha=0 \text{ and } L_1 \text{ Chebyshev Norm,} \\ & J_\alpha(u)_{u \in \mathbb{R}} = |Au - E|_{L_1} + \alpha J(u); \end{aligned} \quad (3)$$

where parameters are defined in Eq. 2. Note the Norm difference with Eq. 2.

Therefore, the main difference between ILS and GA is that in ILS a matrix with dataset is fixed. That matrix A is set to reach the optimal solution u for the system  $Au = E$ , as detailed in Eq. 2. Instead, GA has an extent random set of values that are continuously proved to evaluate their better/worse accuracy subject to constraints. Both methods can be considered useful in optimization. However, GA in recent times has shown get better results specially when functions are more complex, and number of variables and constraints increases. For example, the classical group of GEANT Monte-Carlo software systems resemble GA algorithms in terms of stochastic technique. Monte Carlo and GA methods in general require longer running time [23-37].

There are two main mechanical elements in THA implants, namely, the cup and the head. In bioengineering, the nomenclature is usually CoC (ceramic-on-ceramic, both cup and head), CoM or MoC (ceramic with metal, either). Because of the erosion magnitude and biotribological mechanical/material parameters such as stress, friction, or elasticity modulus, hard bearings are usually CoC, MoC, CoM, or MoM [30]. If at least one polyethylene component is used in THA are included THA is classified as a soft bearings device, such as PoC, MoP or PoP.

All of THA implants have traumatological-clinical advantages and inconvenients, both at operation and

post-operative lifetime. The elective diagnosis for surgical treatment depends of a number of functional factors. These are included in a medical taxonomy [Casesnoves, 2021, 1-4] that has two strands. Namely, clinical factors of the patient (PF), and technical-clinical ones (TCF), which are external to patient itself. PF are varied/individualized, e. g., weight, medical history, age, sex, walk and run activity, associated pathologies, immunological conditions, body frame, overweight, psychological patient-characteristics, etc. TCF are also diverse, mechanical, technical surgical equipment, surgical theatre, surgical staff available, economic requirements of the in-set implants and hospital, instrumentation, etc.

The hip biodynamics depends on two factors, Figure 1 from [1-4]. Firstable the strong muscles to perform the movement, walk and run mainly. Secondly is the strong ligaments group that set the frame-supporting forces to guide-control the contraction/relaxation and also set constraints to avoid-guide and support/prevent/resist any biomechanically-biased movement. Principal ventral muscles for walk and run that create hip rotation cycles are Psoas Major and Minor, Iliacus, Abductor Longis and Adductors system. At dorsal, Gluteus group is essential for locomotion. Main ligaments are Iliofemoral (supporting), Pubofemoral (resisting), Iliolumbar (limiting), and Ischiofemoral (resisting). Grosso modo, hip joint resembles a functional-movement body machine with a wide range of movements/biodynamics. The physiological-anatomical energy is provided by the muscles mechanics, and ligaments/bones constitute the biomechanical skeleton-structure. This human biodynamical system, very similar to primates one, was genetically-optimized during the human evolution along million years with variants depending of human race and earth territory.

According to Europe databases, Germany and Switzerland are the countries with higher number of THA implanted/fixed. Statistically, [1-4], the pathogenesis of the hip fracture and/or hip articulation malfunction corresponds to the high incidence/prevalence of osteoporotic femur neck fracture, Figure 1. This happens usually in elderly-women patients. Factors that increase this

incidence/prevalence increases are the higher average population age, lifetime expectancy, and lack of physical activity. This low physical activity and daily workplace sitting-down time increase causes ligaments and muscles weakness and at late lifetime stages additional osteoporosis [1-4].

Therefore, this contribution presents three main objectives related to Dual Mathematical Optimization of common CoC implant materials. First is the demonstration that both ILS and GA methods verify the results of previous publications [1-4]. Second is to show GA Optimization and ILS improved mathematical algorithms based on Tikhonov functionals. Third is the development of software for 2D, 3D and 4D Graphical and Interior Optimization for the selected model.

In summary, the numerical results of previous contributions are verified numerically and with imaging processing software. Additionally, new mathematical algorithms and computational programming methods are proven. From these Medical Physics findings, emerge a series of numerical data and imaging 3D graphical surfaces to select/compare ceramic materials and get objective parameters database for *in vitro* simulations, manufacturing and/or tribotesting of THA implants.

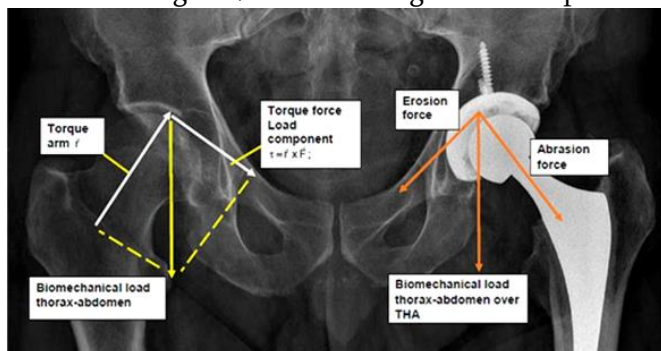


Figure 1.-From previous contributions [1-4], pictured inset-right, the mechanical torque sketch force that summed to biomechanical causes can originate femur neck fracture. On the left, pictured-inset, the biomechanical-dynamical forces distribution that cause erosion, wear, debris and abrasion in the THA device. [Google free images labeled and drawn by author].pictured inset, 2D basic forces distribution in normal hip. Further extent biomechanical details can be found in [1-4].

## II. GENETIC ALGORITHMS NUMERICAL METHOD AND PROGRAMMING

Genetic Algorithms (GA) Optimization Methods have experienced an increase use in recent decades for optimization. It is considered here a practical-brief description of GA method. Actually, there are several GA variants, everyone has its advantages and inconvenients [50,52]. Basically, GA is a stochastic-mixed method similar to Monte Carlo, but faster in general. It is based on computational random successive generations for the objective function. Every generation is subject to elite-selection, after mutations and cross-over changes in variable values. That is the resemblance with the nature genetic evolution for chromosomes [50,52]. As it happened in natural evolution, the generations that show better adaptation (measured with minimum residual magnitude) on the objective function are selected along every optimization step.

There are several important concepts of GA for practical applications in this study. GA method is similar to the random-stochastic Simulated Annealing (SA) method [32-35]. However, SA may be stalled at a local minimum function-concavity because of its algorithm-structure. But GA stops when the tolerance for a chromosome generation is reached, no matter if that solution is a local or global minimum. Instead, Monte Carlo global minimum search is more intensive and evaluates the objective function parameters in search for a global minimum, if it exists, without stopping easily at any local minima. This causes the classical lateness of Monte Carlo compared to other faster optimization methods. In plain language, GA method resembles the discovery for nature evolution created by Darwin in his Selection of Species Theory. That is, the natural evolution generated the random-stochastic genetic combination of DNA-genes in the species reproduction cycle [52]. Those new individuals who showed better survival adaptation continued alive and getting reproduced. Those new individuals who showed bad survival adaptation did not continue alive and getting reproduced. In that way, the best genetic-code of those successful individuals continued being transmitted for future generations,

while the bad genetic-code DNA-combination of the unsuccessful individuals did not survive and was discarded for reproduction-continuity. The consequence was the survival/adaptation of the specie along million years. In other words, the Monte-Carlo and Stochastic Optimization Methods for earth life and biodiversity was invented and optimized by nature million years ago [34,35,52].

For rapid programming with GA in Matlab, it is necessary to call any of available subroutines along the software structure. The accessible options/combinations is quite large/diverse. In this study simple constrained nonlinear optimization is performed. Additionally, Imaging Processing methods constitute a programming part to get informative algorithm graphs.

The algorithms that were implemented previously [1-5] are based on classical Archard's model [5]. A variant from this model with evolved algorithms was developed in previous contributions [Casesnoves, 2018-20,5]. The classical equation for wear optimization of hip implants reads,

$$W = K \frac{L \times X}{H} ; \tag{4}$$

where K is wear constant specific for each material, L biomechanical load (N, passed here to kg and mm), X sliding distance of the acetabular semi-sphere of the implant (mm), and H is the hardness of the implant material (MPa, here it is used always kg and mm). X is measured as the number of rotations of the implant multiplied by approximately half distance of its circular-spherical length. Number of rotations depend of the daily physical activity of the patient, one/several million cycles (Mc), is the standard. Number of rotations is calculated with the circumference implant-head radius R by  $\pi$  for a factor of angle of 145°.

Model (4) is also used in integral form for finite elements techniques in hip implants. For GA, K is the main optimization parameter, hardness, and load are the secondary ones. For Inverse Least Squares, optimization parameters are the same.

Therefore, the OF with L<sub>1</sub> Chebyshev Norm that is used, [Casesnoves Algorithm, 2020-1], without fixed constraints reads,

minimize OF Tikhonov Functional with L<sub>1</sub> Chebyshev Norm,

$$\left| \vec{W} - \vec{K} \frac{\vec{L} \times \vec{X}}{\vec{H}} \right|_{L_1} + \alpha |T|_{L_1} \cong 0 ;$$

subject generically to,

$$\begin{bmatrix} a \\ b \\ c \\ d \\ e \end{bmatrix} \leq \begin{bmatrix} |\vec{K}_i| \\ |\vec{L}_i| \\ |\vec{X}_i| \\ |\vec{H}_i| \\ |\vec{W}_i| \end{bmatrix} \leq \begin{bmatrix} a_1 \\ b_1 \\ c_1 \\ d_1 \\ e_1 \end{bmatrix} ;$$

(5)

where a, b, c and d are constraint parameters to be selected. The parameter  $\alpha$  is selected null. The second term is the Regularization Parameter. All parameters are vectors, K is wear constant specific for each material, L biomechanical load (N, passed here to kg and mm), X sliding distance of the acetabular semi-sphere of the implant (mm), and H is the hardness of the implant material (MPa, here it is used always in kg and mm).

This initial OF equation is algebraically modified when setting in within the program, both for GA and ILS. X is measured as the number of rotations of the implant multiplied by approximately a THA head circular sector corresponding to 145° of the THA head sphere [1-5]. Constrained are a must for optimization, as proven in Proposition 1. W values are experimental *in vitro* figures from the literature, in mm<sup>3</sup> [1-5,26]. The most important one is H, because what is intended is to compare/get practical

optimal results for a dual-group of THA materials. Load parameter is selected within a wide common weight range [50 , 80] kg of patient. That is, from weight of a usual old patient until a common or sporting young person.

The software and mathematical methods of this contribution constitute both a group of improved programs in Volume-matrices arrays-design from previous studies [1-5], and new software for GA.

The GA 3D Interior Optimization is subject to the same constraints of Least Squares 2D Graphical optimization but different [1-4]. That GA program in based on arrays to set a suitable model equation with constraints for optimal GA subroutine configuration. Therefore, numerical GA data can be compared to 2D and 3D Graphical/Interior Optimization of previous Inverse Least Squares results [1-4]. Constraints set results as follows,

$$\begin{aligned}
 &\text{minimize } L_1 \text{ Chevyshev } OF, \\
 &\text{subject to,} \\
 &N = 2 \times 10^6, \\
 &0.02 \leq W \leq 0.1 \text{ mm}^3, \\
 &12 \times 10^6 \leq H \leq 23 \times 10^6 \text{ kg,mm}; \\
 &7.5 \times 10^4 \times 9.8066 \leq L \leq 2.0 \times 10^5 \times 9.8066; \\
 &X = \pi \times 28 \times (145 \times 10^6)/180 \text{ (1 Million cycles)}; \\
 &(6)
 \end{aligned}$$

Table 1 shows the numerical values selected from the literature [1-4, 11]. The implemented numerical data for optimization are CoC hardness (hard bearings) materials, implant head standard diameter [28 mm] , experimental in vitro interval of erosion from literature, and standard units. Additionally, extent complementary data from THA study literature was considered but not used in software design [1-4,7,17,18,21,23,25,27,36].

Table 1.-Materials CoC data implemented in GA and LS optimization model with complementary details.

OPTIMIZATION NUMERICAL DATA		
Material	Hardness (GPa) and Histo-compatibility	Density (g/cm <sup>3</sup> ) and Head Diameter (mm)
Alumina (Al <sub>2</sub> O <sub>3</sub> )	22.0 good	3.98 28 [22-28]
Zirconium (ZrO <sub>2</sub> )	12.2 good	5.56 28 [22-28]
Experimental Wear Interval For Optimization	[ 0.02 , 0.1 ] in mm <sup>3</sup>	
Complementary Data	ElasticityModulus and Fracture Toughness are useful for other type of calculations. Density varies slightly in literature. The standard femoral head used diameter is 28mm. Hardness also varies in literature. For BioloX and BioloX-Delta (ZTA) hardness magnitude varies in the literature.	

Hip implant wear in all the article belongs to cup and prosthesis head together as in [1-5]. Volume parameter is set in mm<sup>3</sup> always, mass in kg, force in N, time in seconds, and the constants of the models applied are function of these units along all study. Force in N is passed on to mm and kg.

Physical/biophysical/biotribological erosion magnitude measurement determination-units of THA implants are specified in different ways along the literature [1-5, 21,25,27]. For *in vitro* research, usually, mm<sup>3</sup> of eroded material per million cycles (Mc) of the femoral head and/or THA cup. For *in vivo*, mass of eroded material per year per Mc, very frequently mm<sup>3</sup> of eroded material extrapolated to one/several years. Otherwise, for *in vivo* studies it is frequent to consider mass or volume of erosion per time interval based in imaging determinations—usually one or several years.

In previous studies [1-4], it was determined approximately what a cycle length for parameter X. Arithmetically, a Mc (a million cycles of femur head

during movement) of rotation length is calculated: circumference implant-head radius R by  $\pi$  for a factor of angle of  $145^\circ$  and by  $10^6$  [1-17].

If/when erosion is measured *in vivo*, other type of units are frequently selected. For example, total volume variation of head and/or cup in mm—that is, the wear-imaging, analytical geometrical comparison at boundaries of a time interval. Usually *in vivo* experimental is rather difficult as non-invasive imaging methods are used/needed.

Load magnitude set in software for optimization constraints is  $\approx 200\%BW$  from literature [1-11,21,25,27,30]. Load constraints for load are magnitudes from a 50 kg patient till a 80 kg patient according to criterion explained in [1-4].

### III. LEAST-SQUARES NUMERICAL METHOD AND PROGRAMMING TECHNIQUES

The software and numerical method of Inverse Least Squares (ILS) algorithm is expressed here with Tikhonov Regularization Algorithms [51]. Programs from previous publications [1-4] with improvements are set with Matlab. 2D Graphical Optimization and 3D Interior Optimization methods [1-4, 23,36]. The programs are based on 3D Volume-Matrices and different in every case, and in this paper designed for sharp comparison to GA method. The ILS inverse algorithm with Regularization Algorithm [Casesnoves, 2021] implemented reads,

minimize OF  $L_2$  and Tikhonov Functional, with  $\alpha = 0$ , such as,

$$\begin{aligned} & \left\| \vec{W} - \vec{K} \frac{\vec{L} \times \vec{X}}{\vec{H}} \right\|_2^2 \cong \dots \\ & \dots = \left\| F(\vec{W}, \vec{K}, \vec{H}, \vec{L}, \vec{X}) \right\|_2^2 + \alpha \left\| T \right\|_2^2 \cong \dots \\ & \dots \cong \sum_{i=1}^{i=N} \sum_{j=1}^{j=N} \dots \\ & \dots \sum_{k=1}^{k=N} \left( F_{ijk} (W_{ijk}, K_{ijk}, H_{ijk}, L_{ijk}, X_{ijk}) \right)^2 + \dots \\ & \dots + F_N (W_{N,N,N}, K_{N,N,N}, H_{N,N,N}, L_{N,N,N}, X_{N,N,N})^2); \end{aligned}$$

subject generically to,

$$\begin{bmatrix} a \\ b \\ c \\ d \\ e \end{bmatrix} \leq \begin{bmatrix} |\vec{K}_i| \\ |\vec{L}_i| \\ |\vec{X}_i| \\ |\vec{H}_i| \\ |\vec{W}_i| \end{bmatrix} \leq \begin{bmatrix} a_1 \\ b_1 \\ c_1 \\ d_1 \\ e_1 \end{bmatrix}; \tag{7}$$

where parameters are defined in Eq. 2. K is the principal variable for optimization. T is Tikhonov matrix, and parameter  $\alpha$  is selected null. Units are set just like in GA algorithm section. For *in vitro* tribopredictions, the usage for dual/multiobjective optimization of an adimensional K parameter makes easier *in vitro* simulations for the THA materials selected.

2D Graphical Optimization is the implementation of this Objective Function (OF), Eq. 7, related to erosion interval and every selected parameter of the model with constraints. N is chosen for an easy running time as  $2 \times 10^6$  functions. The usage of several subroutines combined/complemented with

new patterns was essential to obtain results. In previous papers [1-4], all calculations for every optimal parameter, an approximate/local minimum is determined—global minimum does not exist. For 2D Graphical Optimization, the 3D volume-matrix of the algorithm was converted to a 2D matrix with series of arrays for implementation in patterns.

OF is a nonlinear least squares in Eq. 5. The power 2 of the least squares algorithm converts the objective function into a positive-nonlinear function, and the power (-1) of the hardness model makes it nonlinear within the  $L_2$  Norm. Therefore, OF is an inverse nonlinear LS one, that has provided acceptable results in previous contributions for materials engineering [1-4]. The LS data setting was hardness of ceramic hard-bearings THA types, and loads from Table 1.

With techniques from [1-4], 2D Graphical Optimization graphs/images were done with previously reshaped vectors/matrices set on subroutines [1-4,23,27]. 3D Interior Optimization program for Fig 13 is a new design. Residuals and optimal values for K and the rest of parameters are also obtained in the programs. Erosion experimental magnitude is set in  $\text{mm}^3$ . For ILS constraints are the same than GA program, and read,

$$\begin{aligned} & \text{minimize } L_2 \text{ Norm } OF, \\ & \text{subject to,} \\ & N = 2 \times 10^6, \\ & 0.02 \leq W \leq 0.1 \text{ mm}^3, \\ & 12 \times 10^6 \leq H \leq 23 \times 10^6 \text{ kg,mm}; \\ & 7.5 \times 10^4 \times 9.8066 \leq L \leq 2.0 \times 10^5 \times 9.8066; \\ & X = \pi \times 28 \times (145 \times 10^6)/180 \text{ (1 Million cycles);} \end{aligned} \quad (8)$$

The 2D graphics have surfaces, and simple and/or combined parameter curves whose plotting laborious [1-4]. To obtain a sharp visualization one technique

[1-4], was use scale factors. To get a suitable scale factor, computational trial-error approximations were applied and visualize clearly local minima. Running time for programs results be between 2 and 7 minutes because vectors/matrices have  $2 \times 10^6$  functions. Parameters for 2D Graphical Optimization charts are hardness, load, and model wear.

2D Graphical and 3D Interior Optimization of Figs 9-13 are subject to the same constraints of 2D Graphical Optimization. These programs are based on 2D/3D volume-matrix arrays to set a suitable matrix data configuration. The software is designed to validate images of the previous 2D Graphical Optimization charts [1-4].

#### IV. GA AND LS RESULTS

Results for both programming algorithms are explained along two parts each subsection: numerical results, and 2D, 3D, 4D Graphical and Interior optimization results. 4D Interior Optimization constitute an innovation related to previous contributions [1-4]. The ILS results are an improved review of previous contributions [2,3] with the new 4D Interior Optimization annex-extension. ILS images of 2D and 3D Graphical and Interior optimization are set for comparison from previous studies [2-4].

#### GA RESULTS

Numerical results of applied GA match well the numbers of ILS. Therefore, the ILS data obtained in [1-4] is validated. Table 2 displays GA data obtained by the program. Figures 2-4 show the graphs for best OF fit, average distance among individuals, and stopping criteria for model constraints. Number of generations selected was 500. Figures 5-8 show the 3D Graphical and Interior Optimization charts with matrices of  $10^5$  and  $10^6$  elements. These programs are



rather difficult as it is necessary to link the GA optimization part with the 3D Graphical and Interior Optimization charts. A number of options are available to display the results according to GA theory [50,52]. 4D Interior Optimization is shown and explained specially at Figs 5,6,8.

GA OPTIMIZATION RESULTS		
Material	Optimal K Adimensional For use all parameters in (kg, mm)	Optimal hardness (kg, mm)
ALUMINA	5.9 x 10 <sup>-9</sup> [truncated]	1.5 x 10 <sup>7</sup> [truncated]
ZIRCONUM		In GPA: ≈15.71
Material	Optimal Erosion (mm <sup>3</sup> )	Optimal Load (kg, mm)
ALUMINA	0.03 [truncated]	1.34 x 10 <sup>6</sup> [truncated, kg, mm] If passed to [kg, m, that is Load in kp] 1.34 x 10 <sup>3</sup>

<b>ZIRCONUM</b>	
<b>RESIDUAL FOR OPTIMAL HARDNESS AND ADDITIONAL DATA</b>	2.31 x 10 <sup>3</sup> [truncated, it varies within this magnitude order depending on initial search]  All units used in optimization are passed in Kg and mm. Number of nonlinear function for program is 2 million. The initial Volume-Matrix, that is, a 3D matrix with 3 variables, hardness, load, and experimental magnitudes was converted with programming arrays to a 2D matrix of 2 million functions. Absolute difference between (experimental wear interval)-(model wear interval) ∈ [ 0, 0.08 ] .
<b>GA 3D INTERIOR OPTIMIZATION RESULTS</b>	
3D matrix Program	Validation of K optimal parameter in chart. Validation of erosion rises when Hardness decreases

Table 2.- GA optimization numerical results. Acceptable figures.

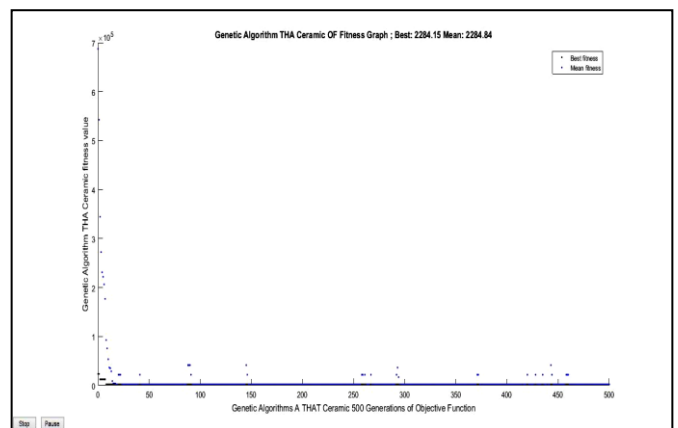


Figure 2.- GA graph of best OF fit. Number of generations was selected 500. In black line, best OF fit. The blue points show the numerical values of generations that converge towards constraints.

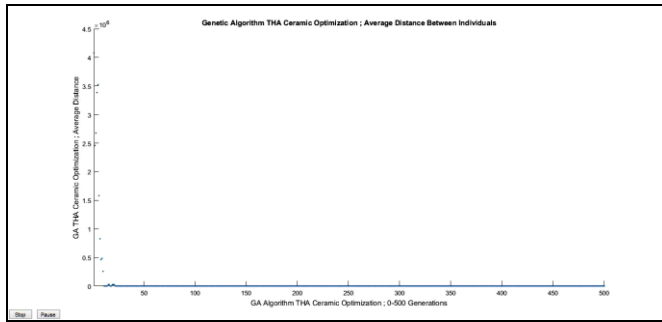


Figure 3.- GA graph of average distance among individuals. Approximately from the 30<sup>th</sup> generation, it is almost null. That confirms the good fitness of the model.

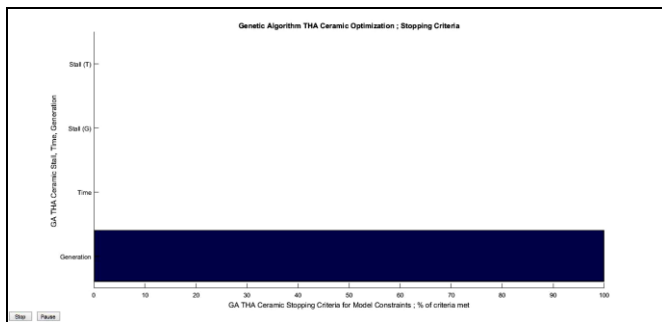


Figure 4.- GA graph of stopping criteria for model constraints. It shows that 100% of criteria is reached with 500 generations.

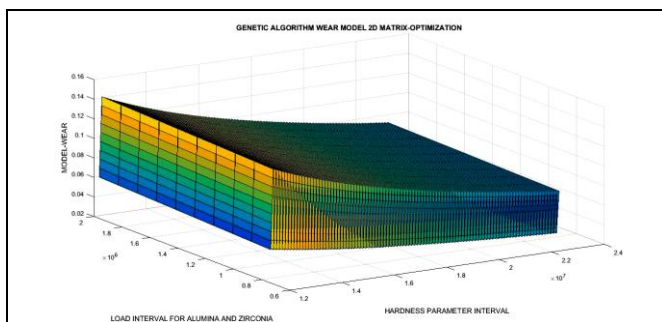


Figure 5.- GA 3D Interior Optimization graph with a 2D matrix for hardness and load with  $10^4$  elements. The optimal K in the graph is given by the GA subroutine. The imaging subroutine is a variant different from [1-4].

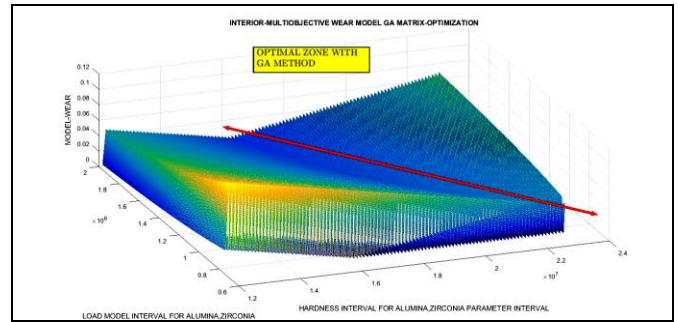


Figure 6.- GA 3D Interior Optimization graph with a 3D matrix for hardness and load with  $10^6$  elements. The optimal K in the graph is given by the GA subroutine. The optimal zone for model values is a diagonal along the surface. In this diagonal, several optimal values of model load and hardness can be selected for different tribological options. The imaging subroutine is a variant different from [1-4]. 4D is the cursor-set along the height of the 3D volume. With that data (hardness, load, wear), the K value in model can be obtained as  $M_c$  is fixed. The image is enhanced at Appendix.

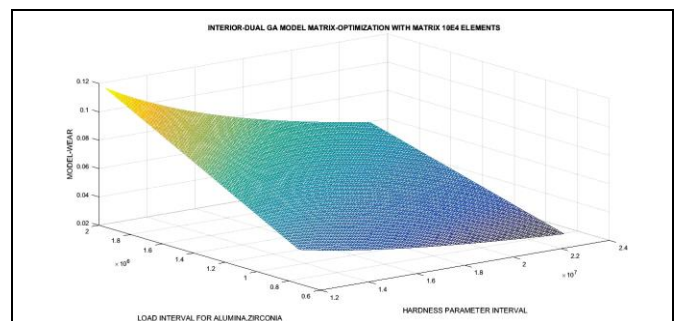


Figure 7.- GA 3D Interior Optimization graph with a 2D matrix for hardness and load with  $10^4$  elements. The optimal K in the Matlab prompt and graph is given by the GA subroutine. The optimal values zone for model values is not marked as previous image for different image setting options. The imaging subroutine is a variant different from [1-4].

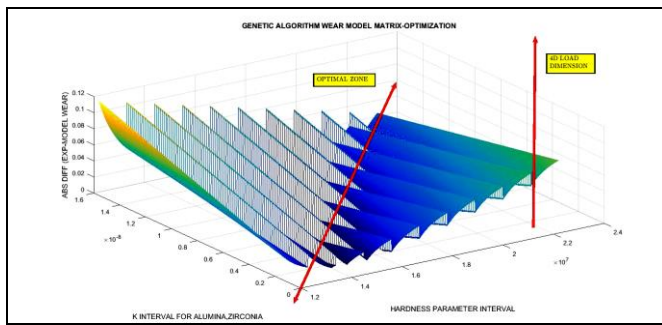


Figure 8.- GA 3D Interior Optimization graph with a 3D matrix for hardness and K interval with  $10^5$  elements. The optimal K in the graph is given by the GA subroutine. 4D Load parameter can be obtained with cursor and model equation. That is, for a given hardness and K value, those peaks show the increase-decrease of the absolute difference between model and wear related to different load variations within load constraint. The optimal zone for model values is a diagonal along the surface. In this diagonal, several optimal values of model K, load and hardness can be selected for different tribological options. The K values along optimal zone match the optimal numerical minima. The imaging subroutine is a variant different from [1-4]. The image is enhanced at Appendix.

For validation of GA optimality of local minima values at the model, it is calculated,

$$\begin{aligned}
 & \left| K(\text{optimal}) \times \frac{\text{Load}(\text{optimal}) \times Mc}{\text{Hardness}(\text{optimal})} \right| = \\
 & = 9.82 \times 10^{-9} \times \frac{1.34 \times 10^6 \times Mc}{1.57 \times 10^7} = \\
 & = 0.0351 \in [0.02, 0.1];
 \end{aligned}
 \tag{9}$$

Therefore, optimal GA numerical values local minima obtained with the graphs/software fall into experimental data interval. The 0.0351 value corresponds approximately to the interval center, and it is seen/guessed also at graphics 5-8. Therefore, GA

numerical result, is not around the experimental interval boundaries, and will match the ILS Eq. 10 results. This implies that for both Alumina and Zirconia materials, the optimal K value obtained by GA and ILS is validated and according to experimental wear magnitudes published [1-7, 21, 26].

### ILS RESULTS

ILS The results developed in [2,3] are shown in Table 3 and Figs 9-13. Optimal hardness to be compared to GA result one was also passed on GPA. Graphics software [2,3] is improved for Fig. 13. Every Figure 9-13 is explained in detail. Local minima for hardness, load, and wear, are presented in Figs 9-12.

The 2D plots and areas correspond to model objective function (Y axis) related to parameter values (X axis). 2D nonlinear optimization matrix in [2] was programmed in an array of  $2 \times 10^6$  functions. To get an acceptable image, Matlab running time is  $\approx 2-7$  minutes [2,3]. Additional explanations of software arrays, loops, patterns, and programming subroutines with selected options can be learnt from [1-4]. Residuals are acceptable for  $2 \times 10^6$  functions in OFs developments. Just remark that units set in model/program are kg and mm. Therefore, to pass results on to International Units System factors are necessary, Table 3. Eq. 10 validates the numerical results.

Table 3.- Dual ILS optimization numerical results. Acceptable figures.

DUAL ILS OPTIMIZATION NUMERICAL RESULTS			
Material	Optimal K adimensional	Optimal hardness (Kg, mm)	Residual
ALUMINA	9.587464 x 10 <sup>-9</sup>	1.526 x 10 <sup>7</sup>	1.76697 x 10 <sup>3</sup>
ZIRCONUM		In GPA: ≈15.27	
Material	Optimal Erosion (mm <sup>3</sup> )	Optimal Load (kg, mm)	Residual
ALUMINA	0.0489	1.099 x 10 <sup>6</sup>	1.76697 x 10 <sup>3</sup>
ZIRCONUM		If passed to [kg, m, that is Load in kp] 1.099 x 10 <sup>3</sup>	
<b>ADDITIONAL DATA</b>	All units used in optimization are passed in Kg and mm. Number of nonlinear function for program is 2 million. The initial Volume-Matrix, that is, a 3D matrix with variables, hardness, load, and experimental magnitudes was converted with programming arrays to a 2D matrix of 2 million functions. Absolute difference between (experimental wear interval) - (model wear interval) ∈ [0, 0.08] .		

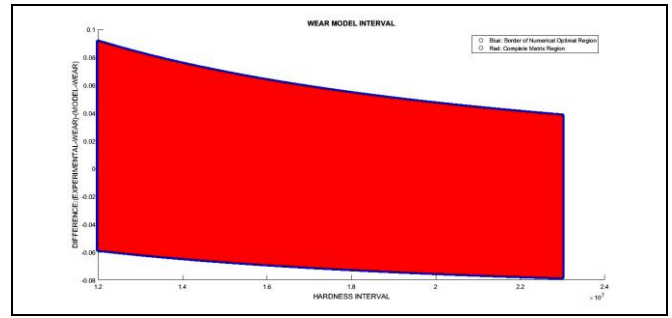


Fig 9.-2D Graphical Optimization chart of model K parameter. The 2 10<sup>6</sup> elements matrix for all programming evaluated parameters fills a 2D region. At Y axis, the difference between model and experimental wear. It is not absolute difference, so it could be also negative. Matrix covers mostly all possible combinations of parameters, namely, load, hardness, and experimental wear. The initial 3D Volume-Matrix with 3 variables, hardness, load, and experimental values, was transformed using arrays to a 2D matrix of 2 10<sup>6</sup> functions. Optimal K is 9.587464 x 10<sup>-9</sup> . Residual is 1.76697 x 10<sup>3</sup> .

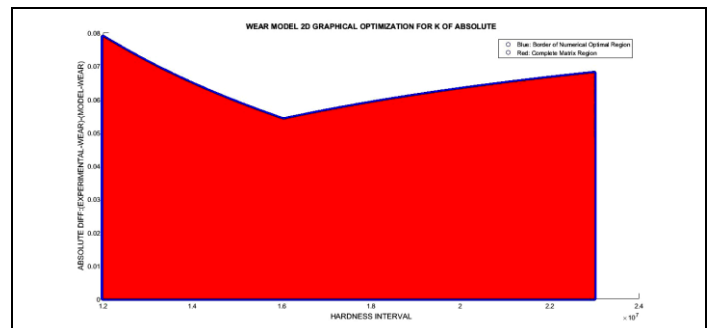


Fig 10.-2D graphical optimization of model for Optimal hardness that can be observed at peak-concavity approximately at 1.5 x 10<sup>7</sup> . At Y axis absolute value of (Experimental -Model) wear magnitude. The 2 10<sup>6</sup> volume-matrix, transformed into 2D, for all evaluated parameters in optimization program covers all 2D region. Matrix covers mostly all possible combinations of parameters, namely, load, hardness, and experimental wear. With 2D Graphical Optimization is exactly 1.526 x 10<sup>7</sup> . Absolute value of (Experimental -Model) wear magnitude falls within interval [0,0.08]. Therefore, an acceptable

result for the experimental data implemented, [0.02, 0.1].

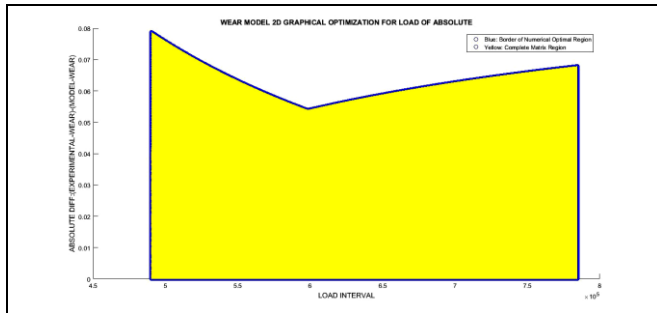


Fig 11.-2D graphical optimization of model for Optimal Load that can be observed at peak-concavity approximately at  $1.5 \times 10^7$ . At Y axis absolute value of (Experimental –Model) wear magnitude. The  $2 \times 10^6$  volume-matrix, transformed into 2D, for all evaluated parameters in optimization program covers all 2D region. Matrix covers mostly all possible combinations of parameters, namely, load, hardness, and experimental wear. With 2D Graphical Optimization is exactly  $1.099 \times 10^3$  N. Absolute value of (Experimental –Model) wear magnitude falls within interval [0,0.08]. Therefore, an acceptable result for the experimental data implemented, [0.02, 0.1]. For higher loads the OF is approximately very similar.

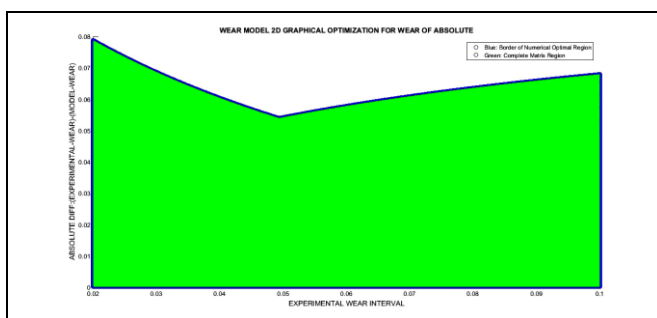


Fig 12.-2D graphical optimization of model for Optimal Wear that can be observed at peak-concavity approximately at  $0.0437 \text{ mm}^3$ . It is a local minimum. At Y axis absolute value of (Experimental –Model) wear magnitude. The  $2 \times 10^6$  volume-matrix, transformed into 2D, for all evaluated parameters in

optimization program covers all 2D region. Matrix covers mostly all possible combinations of parameters, namely, load, hardness, and experimental wear. Absolute value of (Experimental –Model) wear magnitude falls within interval [0,0.08]. Therefore, an acceptable result for the experimental data implemented, [0.02, 0.1].

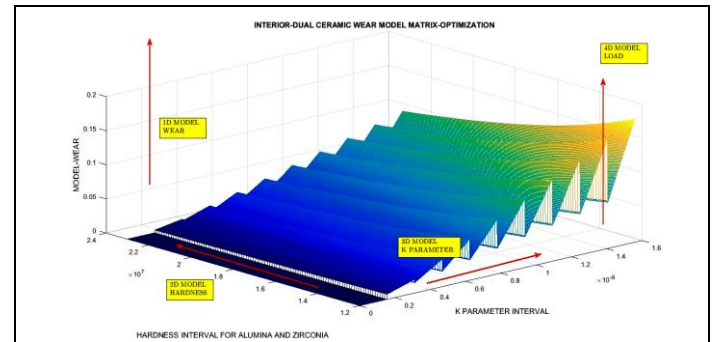


Fig 13.-4D interior optimization of model for 4 dimensions. At Z axis absolute value of model wear magnitude. The dimensions are pictured inset with arrows. Array volume-matrix has  $10^5$  elements. Software was improved from [1-4]. An acceptable result for the experimental data implemented, [0.02, 0.1]. Enhanced in Appendix.

For validation of ILS optimality of local minima values at the model, it is calculated,

$$\left| K(\text{optimal}) \times \frac{\text{Load}(\text{optimal}) \times Mc}{\text{Hardness}(\text{optimal})} \right| = 9.59 \times 10^{-9} \times \frac{1.10 \times 10^6 \times Mc}{1.53 \times 10^7} = 0.0489 \in [0.02, 0.1]; \tag{10}$$

Optimal numerical values local minima obtained with the graphs/software fall into experimental data interval. The 0.04 value corresponds approximately to the interval center, and it is seen also at graphics 9-13. Therefore, numerical result, is not around the

experimental interval boundaries. This implies that for both Alumina and Zirconia materials, the optimal K value obtained is according to experimental wear magnitudes published [1-7, 21, 26].

**V. GA AND ILS COMPARATIVE EVALUATION**

The most important comparative result is the very acceptable match between the two optimization methods. This proves/validates the parameter-optimization of the model. Table 4 shows the evaluation of both methods findings with comments. Both methods, GA and ILS show be accurate. For programming, in general, GA is simpler wit convenient subroutines.

GA AND ILS COMPARATIVE EVALUATION		
METHOD CHARACTERISTIC	GA	ILS
NUMERICAL PRECISION	ALMOST EQUAL	ALMOST EQUAL
PROGRAMMING DIFFICULTY	SIMPLER	MORE DIFFICULT
CONSTRAINTS PROGRAM SETTINGS	SIMPLER	MORE DIFFICULT
MATRICES CONSTRUCTION IN PROGRAM	SIMPLER	MORE DIFFICULT
RUNNING NUMERICAL TIME	LONGER	SHORTER
RUNNING IMAGING PROCESSING TIME	LONGER	SHORTER

Table 4. Evaluation of GA and ILS methods characteristics for this model optimization.

**VI. COMPUTATIONAL-SURGERY AND BIOMECHANICAL APPLICATIONS**

MEDICAL-PHYSICS-BIOENGINEERING APPLICATIONS	
TYPE	USAGE
DESIGN/MANUFACTURING THA IMPLANTS	Simulations in selection/design of materials
EROSION PREDICTION FOR INDIVIDUAL PATIENT	Provided patient characteristics, clinical individual THA type selection before implantation
RESEARCH FOR DIFFERENT/FUTURE THA	Simulations of new similar not limited to ceramic materials
RESEARCH FOR FUTURE CERAMIC THA	The ceramic-composed materials wear whose hardness fall within the computed parameters-interval can also be simulated with these optimal results.
EXTRAPOLATION OF RESULTS FOR OTHER ARTICULATION IMPLANTS	For example, knee implants
THA DURABILITY PREDICTION IN TIME	Provided data of Mc for a time interval, optimal functionality clinical orthopedics lifetime calculations
DIFFERENT MODELS DESIGN MODEL AND PARAMETER OPTIMIZATION IMPROVEMENTS.	Improvements for optimal parameters for hardness, load, and wear efficacy
PRE-OPERATION SIMULATIONS AND POST-SURGERY EVALUATION	Computational simulations for pre-operation THA selection and after surgery THA evaluation

Table 5.-Brief of Medical Physics and Bioengineering applications of study results.

The K adimensional coefficient for similar/equal materials to Alumina and Zirconia with hardness values within their interval shows be useful. Table 5 presents the most important Medical Physics and Bioengineering applications. The optimal model parameters could approximately predict the wear magnitude also for higher number of Mc and different loads within the load interval set. Just to remark that the model fit was made for *in vitro* tribotesting with experimental lab data [1-4].

## VII. DISCUSSION AND CONCLUSIONS

The study objectives were to develop THA ceramic optimization with two mathematical methods in Matlab, and evaluate/compare them. Algorithms are developed with Tikhonov Regularization Theory. This estimation was for numerical results, 2D Graphical Optimization and 3D/4D Interior Optimization. Satisfactorily, the assessment of THA ceramic optimization for LS compared to GA verifies the numerical and graphical results of previous contributions [1-4]. Numerical values of model adimensional K coincide sharply. TR shows be useful for both methods/algorithms. Program structure for GA optimization has less variants compared to LS software code-group. The reason is that with the first series of software designs, high-order matrices and 3D volume-matrices arrays are not necessary. However, GA method requires careful setting of constraints and initial search choice—it was selected 500 generations. In addition, in GA software, the sentences to obtain graphical information imply precise programming. Namely, best OF fit, distance among individuals, and stopping criteria. Moreover, there is a wide range of GA graphics selection to determine the algorithm running features—it is compulsory to select those more numerically significant.

The results importance of the research is that with two different nonlinear optimization methods numerical figures and graphical data coincide

precisely. That is, by using a classical optimization method, LS, and a modern one, GA, the almost same practical parameters were obtained. Just to remark that the model equation is intentionally chosen simple, for fast laboratory *in vitro* biotribotesting [1-4].

Applications in Medical Physics, given the confirmed model parameters with two methods, are theoretical and practical. Theoretical are useful for model future improvements. Practical for THA design tribosimulations *in vitro* and wear prediction of ceramic THA *in vivo*. Medical Physics and Bioengineering extrapolated usages for other similar articulations artificial implants emerge from the investigation results.

## VIII. SCIENTIFIC ETHICS STANDARDS

2D/3D Graphical and Interior Optimization Methods were created by Dr Francisco Casesnoves in December 2016, and Interior Optimization Methods in 2019. 4D Graphical and Interior Optimization Methods were created by Dr Francisco Casesnoves in 2020. This GA new software was originally developed by author. This article has previous paper information, from [2], whose inclusion is essential to make the contribution understandable. The ILS Section Results have the images of [2] because the study is comparative with GA method. The GA nonlinear optimization software was invented/improved from previous contributions in subroutines modifications, patters, loops, graphics and optimal visualization. The 4D Interior Optimization method is original from the author (August 2021). This study was carried out, and their contents are done according to the European Union Technology and Science Ethics. Reference, 'European Textbook on Ethics in Research'. European Commission, Directorate-General for Research. Unit L3. Governance and Ethics. European Research Area. Science and Society. EUR 24452 EN [48,49]. And based on 'The European Code of Conduct for Research Integrity'. Revised Edition. ALLEA. 2017. This research was completely done by the author, the computational-software, calculations, images,

mathematical propositions and statements, reference citations, and text is original for the author. When a mathematical statement, proposition or theorem is presented, demonstration is always included. The article is exclusively scientific, without any commercial, institutional, academic, religious or religious-similar, non-scientific theories political, or economic influence. When anything is taken from a source, it is adequately recognized. Ideas from previous publications were emphasized due to a clarification aim [48,49].

## IX. REFERENCES

- [1]. Casesnoves, F. Mathematical Standard-Parameters Dual Optimization for Metal Hip Arthroplasty Wear Modelling with Medical Physics Applications. *Standards* 2021, 1, 53–66. <https://doi.org/10.3390/standards1010006>.
- [2]. Casesnoves, F. Nonlinear Inverse Dual Optimization for Hip Arthroplasty Ceramic Materials. *AJMS (Asian Journal of Mathematical Sciences)*. Jan-Mar-2021/Vol 5/Issue 1. Pp 53-61. ISSN 2581-3463. 2021.
- [3]. Casesnoves, F. Multiobjective Optimization for Ceramic Hip Arthroplasty with Medical Physics Applications. *Int. J. Sci. Res. Comput. Sci. Eng. Inf. Technol.* 2021, 7, 582–598, ISSN: 2456-3307, <https://doi.org/10.32628/CSEIT21738>.
- [4]. Casesnoves, F. Nonlinear comparative optimization for biomaterials wear in artificial implants technology. In *Proceedings of the Applied Chemistry and Materials Science RTU2018 Conference Proceedings*. Latvia. October 2018.
- [5]. Merola, M.; Affatato, S. Materials for Hip Prostheses: A Review of Wear and Loading Considerations. *Materials* 2019, 12, 495, doi:10.3390/ma12030495.
- [6]. Navarro, N. Biomaterials in orthopaedics. *J. R. Soc. Interface* 2008, 5, 1137–1158, DOI:10.1098/rsif.2008.0151.2008.
- [7]. Bono, V, and Colls. *Revision Total Hip Arthroplasty*. Springer.1999.
- [8]. Abdel, M, Della Valle, C . *Complications after Primary Total Hip Arthroplasty*. Springer. 2017.
- [9]. Learmonth, I . *Interfaces in Total Hip Arthroplasty*. Springer. 2000.
- [10]. Kurtz, S. Advances in Zirconia Toughened Alumina Biomaterials for Total Joint Replacement. *J. Mech. Behav. Biomed. Mater.* 2014, 31, 107–116, doi:10.1016/j.jmbbm.2013.03.022. 2014.
- [11]. Sachin, G.; Mankar, A. Biomaterials in Hip Joint Replacement. *Int. J. Mater. Sci. Eng.* 2016, 4, pp. 113–125, doi:10.17706/ijmse.2016.4.2.113-125.
- [12]. Li, Y.; Yang, C.; Zhao, H.; Qu, S.; Li, X.; Li, Y. New Developments of Ti-Based Alloys for Biomedical Applications. *Materials* 2014, 7, 1709–1800, doi:10.3390/ma7031709.
- [13]. Kolli, R.; Devaraj, A. A Review of Metastable Beta Titanium Alloys. *Metals* 2018, 8, 506, DOI:10.3390/met8070506.
- [14]. Holzwarth, U.; Cotogno, G. *Total Hip Arthroplasty*. JRC Scientific and Policy Reports; European Commission: Brussels, Belgium, 2012.
- [15]. Delimar, D. Femoral head wear and metallosis caused by damaged titanium porous coating after primary metal-on-polyethylene total hip arthroplasty: A case report. *Croat. Med. J.* 2018, 59, 253–257, DOI:10.3325/cmj.2018.59.253.
- [16]. Zhang, M.; Fan, Y. *Computational Biomechanics of the Musculoskeletal System*; CRC Press: Boca Raton, FL, USA, 2015.
- [17]. Dreinhöfer, K.; Dieppe, P.; Günther, K.; Puhl, W. *Eurohip. Health Technology Assessment of Hip Arthroplasty in Europe*; Springer: Berlin/Heidelberg, Germany, 2009.
- [18]. Casesnoves, F. 2D computational-numerical hardness comparison between Fe-based



- hardfaces with WC-Co reinforcements for Integral-Differential modelling. *Trans. Tech.* 2018, 762, 330–338, DOI:10.4028/www.scientific.net/KEM.762.330. ISSN: 1662-9795.
- [19]. Hutchings, I.; Shipway, P. *Tribology Friction and Wear of Engineering Materials*, 2nd ed.; Elsevier: Amsterdam, The Netherlands, 2017.
- [20]. Shen, X.; Lei, C.; Li, R. Numerical Simulation of Sliding Wear Based on Archard Model. In *Proceedings of the 2010 International Conference on Mechanic Automation and Control Engineering*, Wuhan, China, 26–28 June 2010. DOI:10.1109/MACE.2010.5535855.
- [21]. Affatato, S.; Brando, D. *Introduction to Wear Phenomena of Orthopaedic Implants*; Woodhead Publishing: Sawston, UK, 2012.
- [22]. Matsoukas, G.; Kim, Y. Design Optimization of a Total Hip Prosthesis for Wear Reduction. *J. Biomech. Eng.* 2009, 131, 051003.
- [23]. Casesnoves, F.; Antonov, M.; Kulu, P. Mathematical models for erosion and corrosion in power plants. A review of applicable modelling optimization techniques. In *Proceedings of RUTCON2016 Power Engineering Conference*, Riga, Latvia, 13th October. 2016.
- [24]. Galante, J.; Rostoker, W. Wear in Total Hip Prostheses. *Acta Orthop. Scand.* 2014, 43, 1–46, DOI:10.3109/ort.1972.43.suppl-145.01.
- [25]. Mattei, L.; DiPuccio, F.; Piccigallo, B.; Ciulli, E. Lubrication and wear modelling of artificial hip joints: A review. *Tribol. Int.* 2011, 44, 532–549.
- [26]. Jennings, L. Enhancing the safety and reliability of joint replacement implants. *Orthop. Trauma* 2012, 26, 246–252.
- [27]. Casesnoves, F. *Die Numerische Reuleaux-Methode Rechnerische und Dynamische Grundlagen mit Anwendungen (Erster Teil)*; Scientia Scripta: 2019; ISBN-13: 978-620-0-89560-8, ISBN-10: 6200895600.
- [28]. Casesnoves, F. *Mathematical Models and Optimization of Erosion and Corrosion*. Ph.D. Thesis, Taltech University, Tallinn, Estonia. 14 December. 2018. ISSN 25856898.
- [29]. Saifuddin, A.; Blease, S.; Macsweeney, E. Axial loaded MRI of the lumbar spine. *Clin. Radiol.* 2003, 58, 661–671.
- [30]. Damm, P. *Loading of Total Hip Joint Replacements*. Ph.D. Thesis, Technischen Universität, Berlin, Germany, 2014.
- [31]. Casesnoves, F. *The Numerical Reuleaux Method, a Computational and Dynamical Base with Applications. First Part*; Lambert Academic Publishing: 2019; Republic of Moldava. ISBN-10 3659917478.
- [32]. Casesnoves, F. *Large-Scale Matlab Optimization Toolbox (MOT) Computing Methods in Radiotherapy Inverse Treatment Planning*. High Performance Computing Meeting; Nottingham University: Nottingham, UK, 2007.
- [33]. Casesnoves, F. A Monte-Carlo Optimization method for the movement analysis of pseudo-rigid bodies. In *Proceedings of the 10th SIAM Conference in Geometric Design and Computing*, San Antonio, TX, USA, 4–8 November 2007; Contributed Talk.
- [34]. Casesnoves, F. 1.-‘Theory and Primary Computational Simulations of the Numerical Reuleaux Method (NRM)’, Casesnoves, Francisco. *Int. J. Math. Computation.* 2011, 13, pp. 89-111. Available online: <http://www.ceser.in/ceserp/index.php/ijmc/issue/view/119> (accessed on 28 June 2021).
- [35]. Casesnoves, F. Applied Inverse Methods for Optimal Geometrical-Mechanical Deformation of Lumbar artificial Disks/Implants with Numerical Reuleaux Method. *2D Comparative Simulations and Formulation. Comput. Sci. Appl.* 2015, 2, 1–10. Available online:

www.ethanpublishing.com (accessed on 28 June 2021).

- [36]. Casesnoves, F. Inverse methods and Integral-Differential model demonstration for optimal mechanical operation of power plants–numerical graphical optimization for second generation of tribology models. *Electr. Control Commun. Eng.* 2018, 14, 39–50, DOI:10.2478/ecce-2018-0005.
- [37]. Casesnoves, F.; Surzhenkov, A. Inverse methods for computational simulations and optimization of erosion models in power plants. In *Proceedings of the IEEE Proceedings of RUTCON2017 Power Engineering Conference*, Riga, Latvia, 5 December 2017. doi:10.1109/RTUCON.2017.8125630. Electronic ISBN:978-1-5386-3846-0. USB ISBN: 978-1-5386-3844-6. ISBN: 978-1-5386-3847-7.
- [38]. Abramowitz, S. *Handbook of Mathematical Functions*. Appl. Math. Ser. 55. 1972.
- [39]. Luenberger, G.D. *Linear and Nonlinear Programming*, 4th ed.; Springer: Berlin/Heidelberg, Germany, 2008.
- [40]. Casesnoves, F. Exact Integral Equation Determination with 3D Wedge Filter Convolution Factor Solution in Radiotherapy. *Series of Computational-Programming 2D-3D Dosimetry Simulations*. *Int. J. Sci. Res. Sci. Eng. Technol*, pp. 699-715. 2016, 2.
- [41]. Panjabi, M.; White, A. *Clinical Biomechanics of the Spine*. Lippincott 1980, 42, S3.
- [42]. Casesnoves, F. *Software Programming with Lumbar Spine Cadaveric Specimens for Computational Biomedical Applications*. *Int. J. Sci. Res. Comput. Sci. Eng. Inf. Technol.* 2021, 7, 7–13, ISSN: 2456-3307.
- [43]. Surzhenkov, A.; Viljus, M.; Simson, T.; Tarbe, R.; Saarna, M.; Casesnoves, F. Wear resistance and mechanisms of composite hardfacings at abrasive impact erosion wear. *J. Phys.* 2017, 843, 012060, doi:10.1088/1742-6596/843/1/012060.
- [44]. Casesnoves, F. *Computational Simulations of Vertebral Body for Optimal Instrumentation Design*. *ASME J. Med. Devices* 2012, 6, 021014, <http://dx.doi.org/10.1115/1.4006670>.
- [45]. Barker, P. The effect of applying tension to the lumbar fasciae on segmental flexion and extension. In *Proceedings of 5th International Congress of Low Back and Pelvic Pain*, Melbourne, Australia, 10–13 November 2014; pp. 50–52.
- [46]. Galme, S.; Barker, P.; Bhalerao, Y. *Biomaterials in Hip Joint Replacement*. *Int. J. Mater. Sci. Eng.* 2016, 4, 113–125.
- [47]. *European Textbook on Ethics in Research*. European Commission, Directorate-General for Research. Unit L3. Governance and Ethics. European Research Area. Science and Society. EUR 24452 EN. Available online: <https://op.europa.eu/en/publication-detail/-/publication/12567a07-6beb-4998-95cd-8bca103fcf43>. (accessed on 28 June 2021).
- [48]. ALLEA. *The European Code of Conduct for Research Integrity*, Revised ed.; ALLEA: Berlin Barndenburg Academy of Sciences. 2017.
- [49]. Haupt, R, Haupt, S. *Practical Genetic Algorithms*. Wiley. Second Edition. 2004.
- [50]. Kazufumi, I; Bangti, J. *Inverse Problems, Tikhonov Theory and Algorithms*. *Series on Applied Mathematics Volume 22*. World Scientific. 2015.
- [51]. Darwin, C. *The origin of species*. Barnes & Noble Classics. 2004.

## X. AUTHOR'S BIOGRAPHY

Dr Francisco Casesnoves earned the Engineering and Natural Sciences PhD by Tallinn University of Technology (started thesis in 2016, thesis defence/PhD earned in December 2018, official graduate Diploma 2019), and in computational-engineering/physics. Dr Casesnoves currently is independent research scientist. He earned MSc-BSc, Physics/Applied-Mathematics (Public Eastern-Finland-University, MSc Thesis in Radiotherapy Treatment Planning Optimization, which was developed after graduation in a series of Radiation Therapy Optimization-Modelling publications [2007-present] ), Graduate-with-MPhil, in Medicine and Surgery (Public Madrid University Medicine School, MPhil in Radioprotection Low Energies Dosimetry). Casesnoves studied always in public-educational institutions. Casesnoves resigned definitely to his original nationality in 2020 for ideological reasons, democratic-republican ideology, and ethical-professional reasons, and does not belong to Spain Kingdom anymore. His constant service to

International Scientific Community and Estonian technological progress (2016-present) commenced in 1985 with publications in Medical Physics, with further specialization in optimization methods in 1997 at Finland—at the moment approximately 100 recognized publications with approximately 62 DOI papers. His main branch is Computational-mathematical Nonlinear/Inverse Methods Optimization. Casesnoves best-achievements are the Numerical Reuleaux Method in dynamics and nonlinear-optimization [books 2019-2020], the Graphical and Interior Optimization Methods [2016-8], the new Computational Dissection-Anatomical Method, [2020] and invention of Forensic Robotics [2020-2021]. Dr Casesnoves scientific service since 2016 to the Free and Independent Republic of Estonia for technological development (and also at Riga technical University, Power Electrical and Electronics Department) is about 35 physics-engineering articles, two books series, and 1 industrial radiotherapy project associated to Europe Union EIT Health Program (Tartu University, 2017).

## APPENDICES

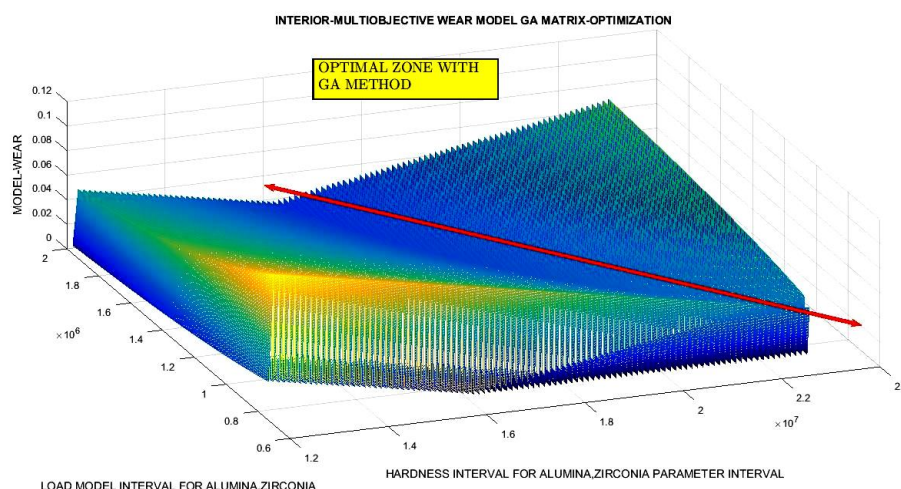


Figure 6-Enhanced.- GA 3D Interior Optimization graph with a 3D matrix for hardness and load with  $10^6$  elements. The optimal K in the graph is given by the GA subroutine. The optimal zone for model values is a diagonal along the surface. In this diagonal, several optimal values of model load and hardness can be selected for different tribological options. The imaging subroutine is a variant different from [1-4]. 4D is the cursor-set along the height of the 3D volume. With that data (hardness, load, wear), the K value in model can be obtained as Mc is fixed.

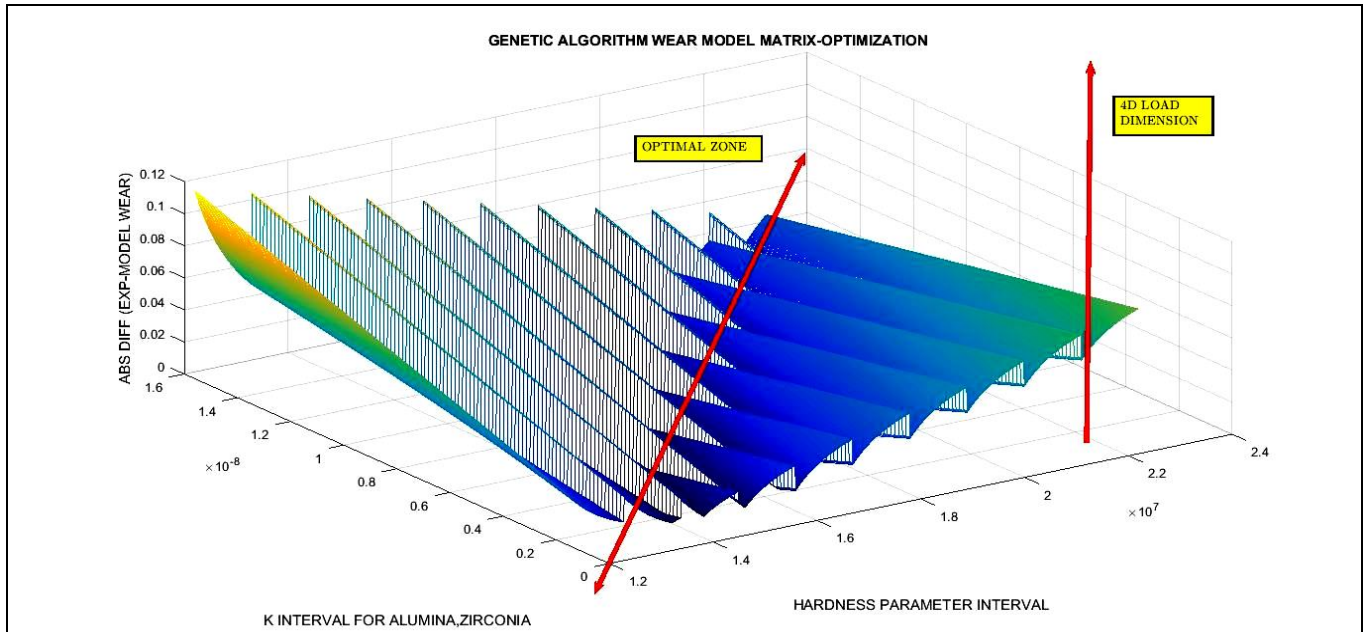


Figure 8-Enhanced.- GA 3D Interior Optimization graph with a 3D matrix for hardness and K interval with  $10^5$  elements. The optimal K in the graph is given by the GA subroutine. 4D Load parameter can be obtained with cursor and model equation. That is, for a given hardness and K value, those peaks show the increase-decrease of the absolute difference between model and wear related to different load variations within load constraint. The optimal zone for model values is a diagonal along the surface. In this diagonal, several optimal values of model K, load and hardness can be selected for different tribological options. The K values along optimal zone match the optimal numerical minima. The imaging subroutine is a variant different from [1-4].

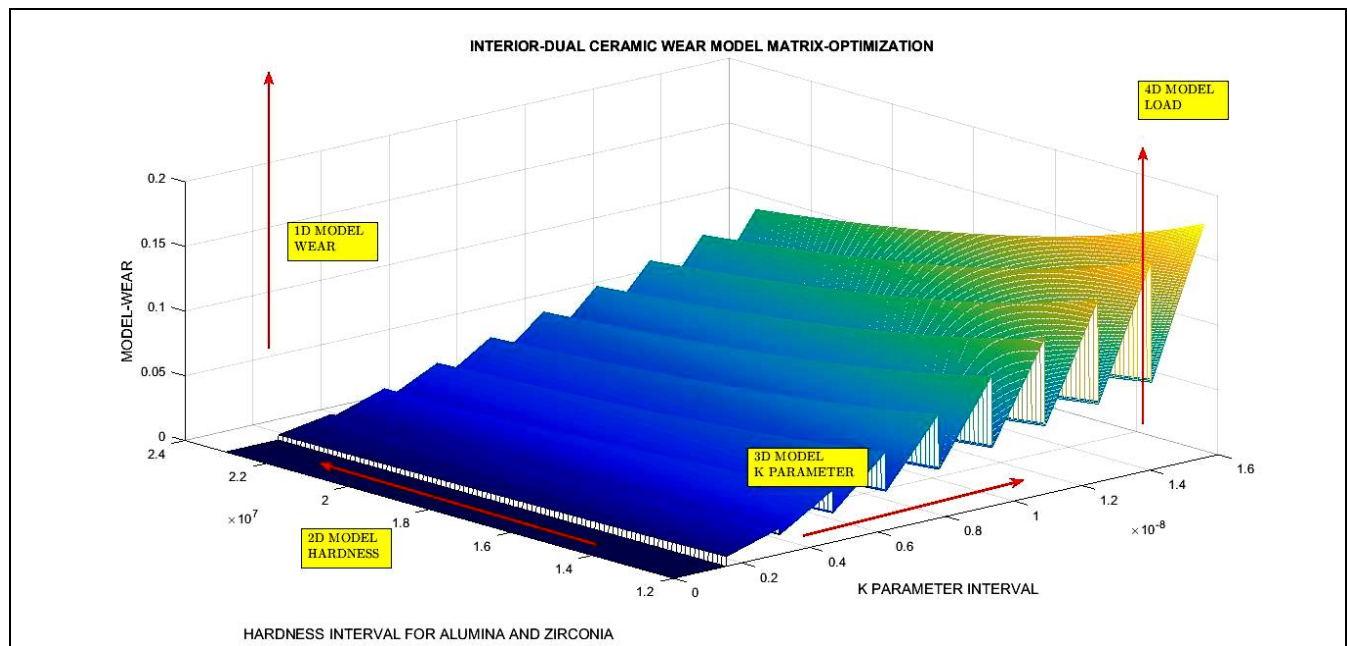


Fig 13-Enhanced.-4D interior optimization of model for 4 dimensions. At Z axis absolute value of model wear magnitude. The dimensions are pictured inset with arrows. Array volume-matrix has  $10^5$  elements. Software was improved from [1-4]. An acceptable result for the experimental data implemented, [0.02, 0.1]. Enhanced in Appendix.

**Cite this Article :**

Francisco Casesnoves , "Genetic Algorithm to Inverse Least Squares Comparative Dual Optimization for Ceramic Hip Arthroplasty in Medical Physics ", International Journal of Scientific Research in Computer Science, Engineering and Information Technology (IJSRCSEIT), ISSN : 2456-3307, Volume 8 Issue 1, pp. 88-108, January-February 2022. Available at doi : <https://doi.org/10.32628/CSEIT2176101>  
 Journal URL : <https://ijsrcseit.com/CSEIT2176101>